Legends for Supplementary Figures

Supplementary Figure 1. Generation of *Anks6*$^{tm1a/tm1a}$ mice.

(**a**) Schematic demonstrating the *Anks6*^{tm1a} allele used in this work. Binding positions of the genotyping primers are indicated with arrows. FRT, flippase recognition target; En2SA, *Engrailed2,* splice acceptor; IRES, internal ribosomal entry site; lacZ, *beta-galactosidase* gene; loxP, loxP sequence; neo, neomycin resistance gene.

(**b**) Genotyping details. Primer positions are shown in (**a**).

(**c**) Genotyping PCR products from tail tips. Primers 636 and 637 generate a 480 bp product from wild type allele, primers 606 and 637 generate 278 bp product from the mutant allele. H_2O, water control.

(**d**) Western blot analysis on *Anks6*$^{+/+}$, *Anks6*$^{+/tm1d}$ and *Anks6*$^{tm1d/tm1d}$ embryo lysates confirms the absence of Anks6 protein from *Anks6*$^{tm1d/tm1d}$ animals. No spurious truncated or full-length forms of Anks6 protein are produced by the *Anks6*^{tm1d} allele. β-actin was used as a loading control.

(**e**) The expression of *gamma-aminobutyric acid type b receptor subunit 2* (*Gabbr2*) gene is unchanged in wild type and *Anks6* mutant E18.5 livers. All experiments are n=5. Two-tailed unpaired t-test was used for statistical analysis. Data are mean and SEM. ns p=0.79. Mean of wild type - 0.88 vs. mean of *Anks6* mutant - 0.93.

(**f**) The expression of *polypeptide n-acetylgalactosaminyltransferase 12* (*Galnt12*) gene is unchanged in wild type and *Anks6* mutant E18.5 livers. All experiments are n=5. Two-tailed unpaired t-test was used for statistical analysis. Data are mean and SEM. ns p=0.93. Mean of wild type - 0.86 vs. mean of *Anks6* mutant - 0.87.

Supplementary Figure 2. Characterization of cardiac phenotypes in *Anks6*$^{-/-}$ mice.

(**a**,**b**) H&E staining of the coronal sections of the control mouse heart at P0, show normal structure of the heart (**a**). In contrast, muscular ventricular septal defect (VSD) is visible in the *Anks6* mutant heart (**b**, arrow). RV, right ventricle; LV, left ventricle.

(**c**) Coronal micro-MRI imaging reveals a spectrum of complex congenital heart malformations in *Anks6*

mutant embryos at E18.5. Embryo #3, has SS, with overriding aorta (red arrow); #7 has HTX, with AVSD (green arrow), overriding aorta (red arrow) and straight arch; #24 has HTX; #21 has SS, with VSD, bilateral ventricular hypertrophy and overriding aorta (red arrow). AVSD, atrioventricular septal defect, HTX, heterotaxia; SS, Situs solitus; VSD, ventricular septal defect.

Supplementary Figure 3. HE staining of *Anks6*$^{-/-}$ liver reveals normal morphology and histology at E15.5.

(**a**,**b**) The liver morphology appears largely unaffected in E15.5 *Anks6*$^{-/-}$ embryos. Note the comparable size of the liver lobes between the wild type (**a**) and *Anks6*$^{-/-}$ (**b**) littermates on a frontal section.

(**c**,**d**) Similarly, the histology of the hilar region appears comparable between wild type (**c**) and mutant (**d**) liver at E15.5. Asterisk marks the stomach, whose position is reversed in *Anks6*$^{tm1d/tm1d}$ mice. Li, liver; Ki, kidney; pv, portal vein. Scale bar, 50 μm.

Supplementary Figure 4. αSMA expression is unchanged in *Anks6*$^{-/-}$ livers at E15.5.

(**a**-**b''**) Staining of wild type (**a**-**a''**) and Anks6 mutant (**b**-**b''**) livers with antibodies against aSMA (red) and Sox9 (green) did not reveal overt changes in the presence of aSMA+ myofibroblasts in the mutant livers compared to wild type livers at E15.5. Sox9+ bile duct progenitors were detected in the livers of both genotypes, although their numbers was reduced in the mutant portal area. pv, portal vein. Scale bar, 50 μm.

Supplementary Figure 5. *Anks6* mutant mice present a spectrum of liver portal defects.

(**a**) The portal mesenchyme is significantly reduced in *Anks6* mutant livers, compared to wild type livers, both at E18.5 and at birth (P0). Portal mesenchyme thickness measured as indicated by red brackets at **Figure 2a**, **d**, **j**, **g**.

(**b**–**e**) *Anks6*$^{-/-}$ bile ducts display degenerative histology in the liver periphery at P0. The portal vein is often completely obliterated and difficult to identify (**a**,**b**,**c**). Numerous collapsed bile duct rudiments surround

the portal vein. Near continuous, unremodelled ductal plate is visible in **e**. Asterisk marks the obliterated portal vein; dashed yellow lines mark the atrophic bile ducts; pv, portal vein. Scale bar, 50 μm.

Supplementary Figure 6. Wnt target gene expression is unchanged in *Anks6*-mutant livers at E18.5.

(**a**) The expression of canonical Wnt targets is unchanged in *Anks6*$^{-/-}$ livers at E18.5. The expression of *Axin2* (ns, p=0.67), *cMyc* (ns, p=0.57) and *Ccnd1* (ns, p=0.14) was measured in wild type (n=5 or 6) and mutant (n=5) total liver lysates by qRT-PCR. Two-tailed unpaired t-test was used for statistical analysis. Data are mean and SEM.

(**b**) The expression of non-canonical Wnt targets is unchanged in *Anks6*$^{-/-}$ livers at E18.5. The expression of *Wnt5a* (ns, p=0.99) and *Dkk1* (ns, p=0.46) was measured in wild type (n=6) and mutant (n=5) total liver lysates by qRT-PCR. Two-tailed unpaired t-test was used for statistical analysis. Data are mean and SEM.

a

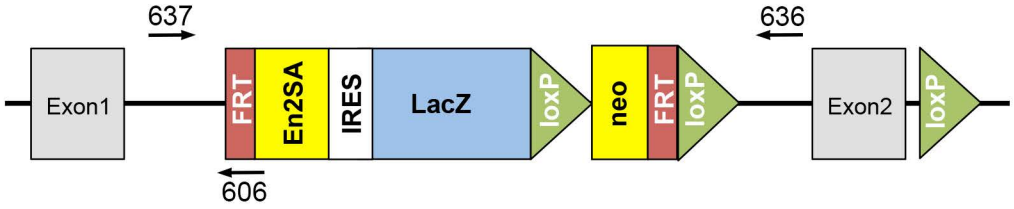

b

606 GGAACTTCGGAATAGGAACTTC
636 CCCATAGACATGCAAACATGC
637 GCAGAGTGGTATAGGCAGATGG

636/637: 480 bp, wild type allele
606/637: 278 bp, mutant allele

c

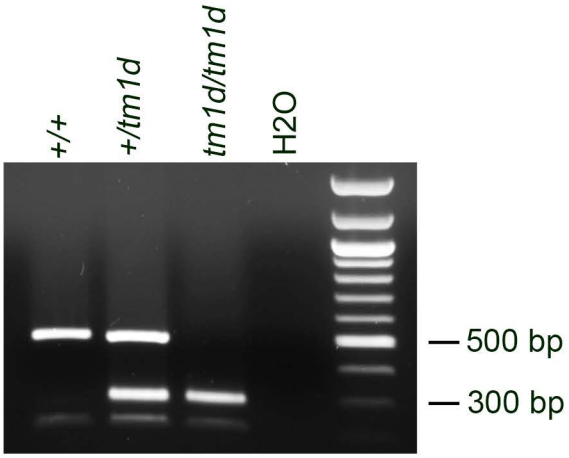

d

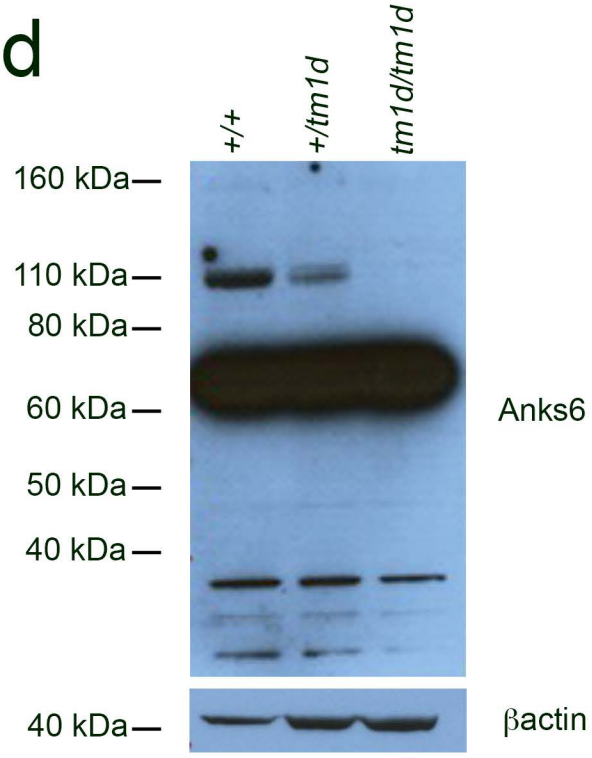

e

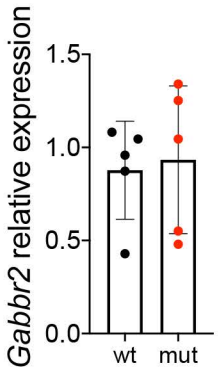

f

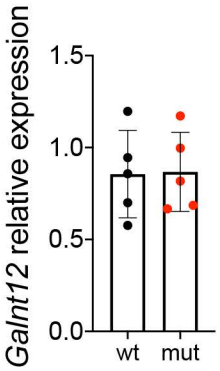

Supplementary Figure 1

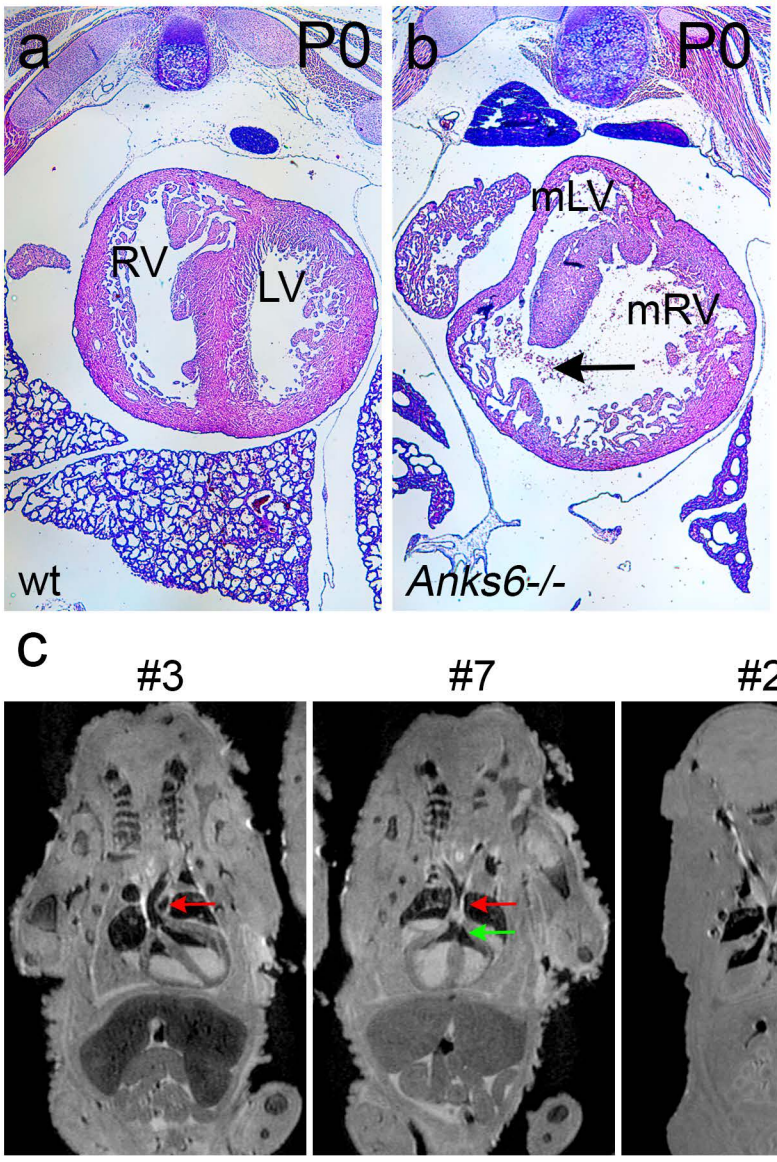

Supplementary Figure 2

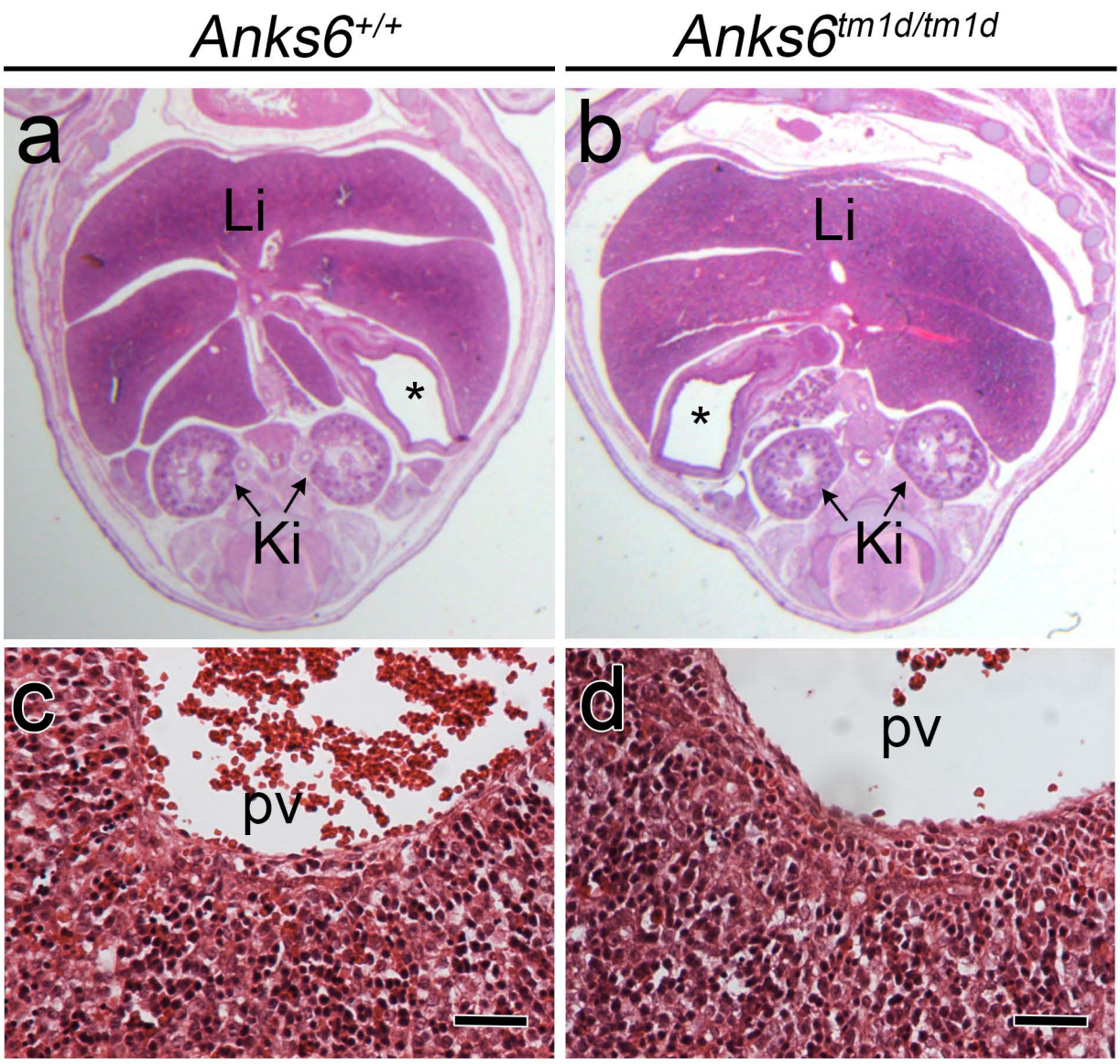

Supplementary Figure 3

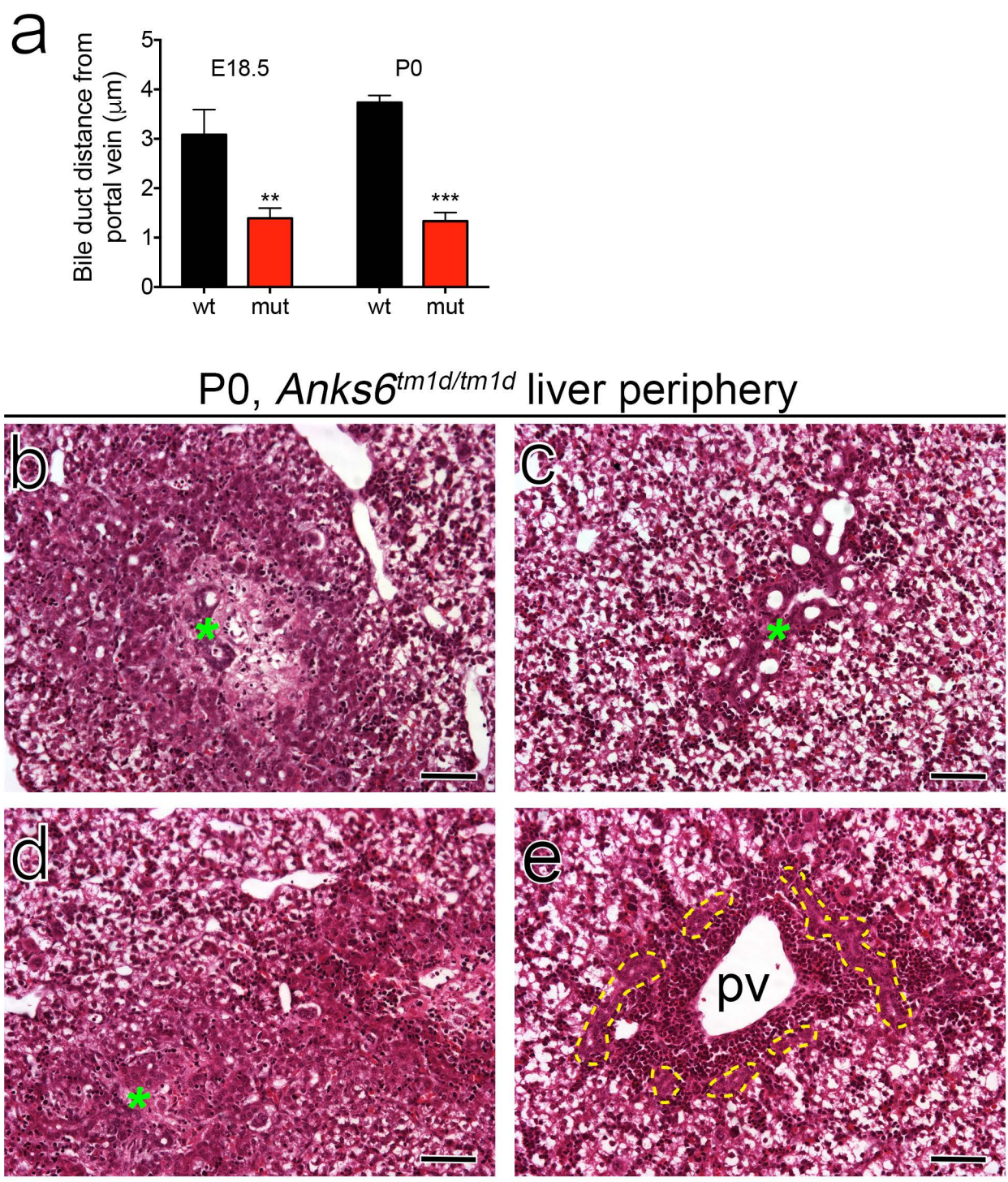

Supplementary Figure 4

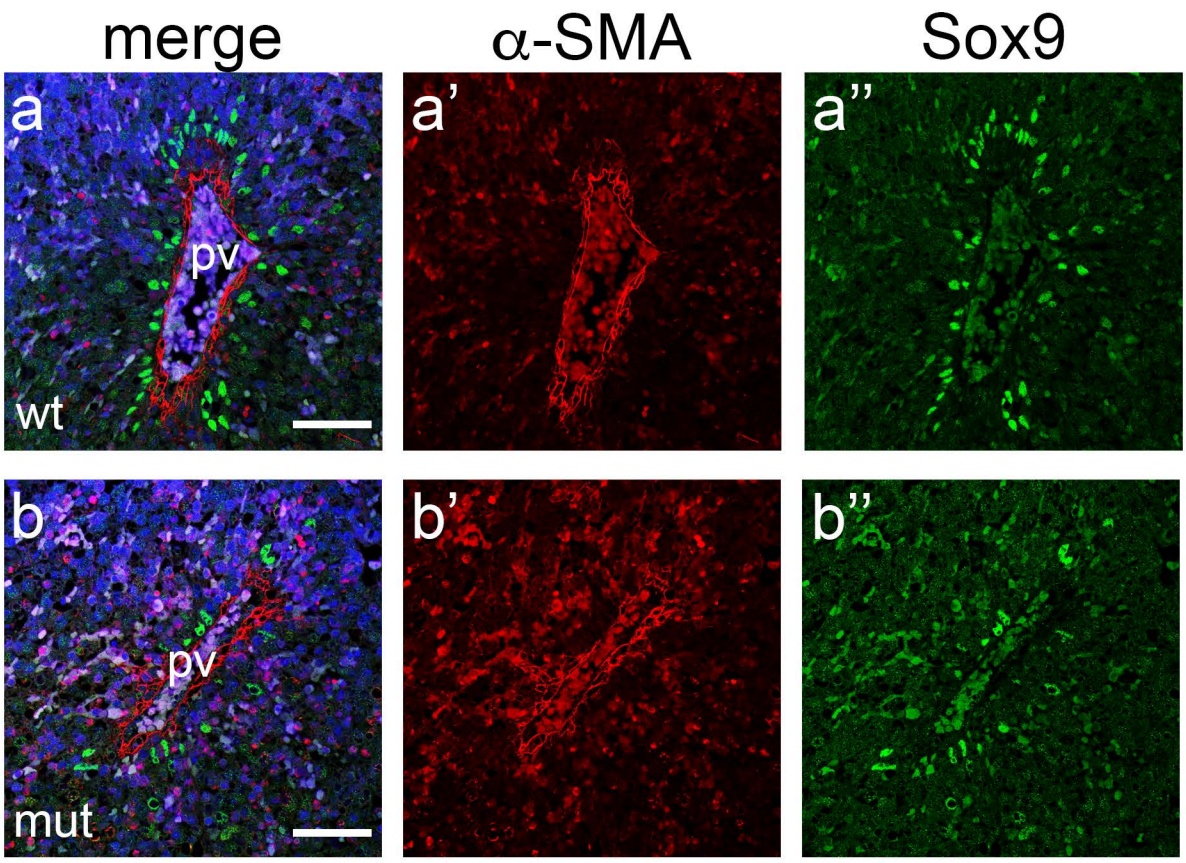

Supplementary Figure 5

a canonical Wnt target genes

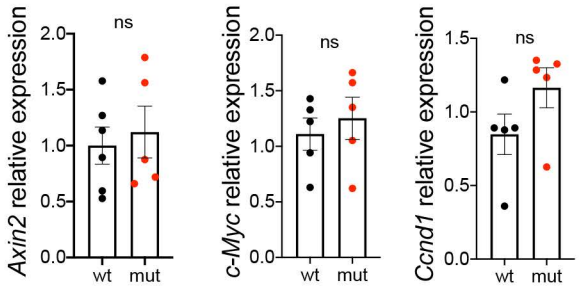

b non-canonical Wnt target genes

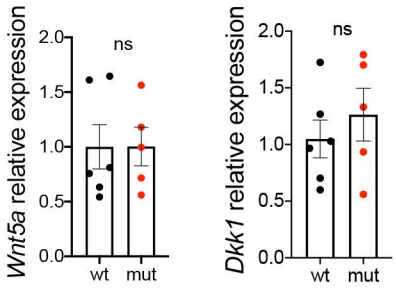

Supplementary Figure 6

Supplementary Table 1. Antibodies and lectins used in the study.

Antibody	Source	Identifier
Mouse anti-β-actin	Abcam	ab49900
Rabbit anti-Albumin	Novus Biologicals	NB600-41532
Mouse anti-ANKS6	Santa Cruz	sc-515124
Rabbit anti-ANKS6	Sigma-Aldrich	HPA008355-100UL
Mouse anti-β-Catenin	BD Transduction Laboratories	610154
Rabbit anti-Cyr61	Abcam	ab24448
Mouse E-cadherin	BD Transduction Laboratories	610182
Mouse anti-EpCAM (CD326)	BioLegend	118205
Mouse anti-FLAG	Proteintech	66008-2-Ig
Rabbit anti-FLAG	Proteintech	20543-1-AP
Mouse anti-Gapdh	Trevigen	2275-PC-100
Rabbit anti-HNF1b	Proteintech	12533-1-AP
Goat anti-INVS	Santa Cruz	sc-8719
Mouse anti-Osteopontin	R&D Systems	AF808
Mouse anti-pan-cytokeratin	Sigma-Aldrich	c2562
Mouse anti-αSMA	Sigma-Aldrich	A5228
Mouse anti-αSMA-Cy3	Sigma-Aldrich	C6198
Rabbit anti-Sox9	Millipore	AB5535
Rabbit anti-acetylated α-tubulin	Cell Signaling	#5335
Mouse anti-gamma-tubulin	Abcam	
Mouse anti-polyglutamylated tubulin	Adipogen	GT335
Rabbit anti-V5	Cell Signaling	#13202
Mouse anti-YAP	Santa Cruz	sc-101199
DBA lectin	VectorLaboratories	B-1035

Supplementary Table 2. qRT-PCR primers used in this study.

Gene	Species	Forward	Reverse
Anks6	mouse	CAACAGCCGCAACCACTAC	GCCTCTAGCAGCAGCTTCAC
Gapdh	mouse	GACTTCAACAGCAACTCCCA	TGTAGCCGTATTCATTGTCATACC
Yap	mouse	TACTGATGCAGGTACTGCGG	TCAGGGATCTCAAAGGAGGAC
Ctgf	mouse	ATGATGCGAGCCAACTGCCTG	CGGATGCACTTTTTGCCCTTCTTAATG
Cyr61	mouse	GTGCCGCCTGGTGAAAGAGA	GCTGCATTTCTTGCCCTTTTTTAG
Sox9	mouse	ACTCTGGGCAAGCTCTGGAG	CGAAGGGTCTCTTCTCGCTCT
Albumin	mouse	GCTGAGACCTTCACCTTCCA	TCTTCAGTTGCTCCGCTGTA
Cytokeratin19	mouse	CCCACGTGTTCCACAAACATC	CCATGGGAACAGTTATTTGGAGA
Fabp2	mouse	GTGGAAAGTAGACCGGAACGA	CCATCCTGTGTGATTGTCAGTT
Axin2	mouse	ACAGCATCTTCACCACTT	AGAAACCCTCACTTCCTAAA
Ccnd1	mouse	CCCAACAACTTCCTCTCCTG	TCCAGAAGGGCTTCAATCTG
cMyc	mouse	CAACGACAGCAGCTCGCCCA	CCGTGGGGAGGACTCGGAGG
Wnt5a	mouse	ACACAACAATGAAGCAGGCCGTAG	GGAGTTGAAGCGGCTGTTGACC
Dkk1	mouse	CGCTGCATGAGGCACGCTAT	GGCGGCGTTGTGGTCATTAC
Gabbr2	mouse	AAGACCCCATAGAGGACATCAA	GGGTGGTACGTGTCTGTGG
Galnt12	mouse	TCAACATCTATCTGAGCGACCG	CTTGGGCAGGTTATCATAATCGT
shRNA target sequences			
Anks6	mouse	CCGGAGCTCGATGTTCTCCCTAATGCTCGAGCATTAGGGAGAACATCGAGCTTTTTTG	
sgRNA target sequences			
Anks6 1-18 (exon1)	mouse	GCGGTCGAGAGCAACCTCGAAGG	
Anks6 2-15 (exon2)	mouse	CCTGTACTTGCGGTCGAGAGCAA	